Korean J. Chem. Eng., 39(10), 2800-2809 (2022)
DOI: 10.1007/s11814-022-1156-6

pISSN: 0256-1115
eISSN: 1975-7220

Modeling and optimization of dynamic viscosity of oil-based nanofluids containing alumina particles and carbon nanotubes by response surface methodology (RSM)

Mohammad Hemmat Esfe*, Sayyid Majid Motallebi, and Davood Toghraie***,†**

*Department of Mechanical Engineering, Imam Hossein University, Tehran, Iran
**Department of Chemical Engineering, Imam Hossein University, Tehran, Iran
***Department of Mechanical Engineering, Khomeinishahr Branch, Islamic Azad University, Khomeinishahr, Iran
(*Received 26 December 2021 • Revised 16 April 2022 • Accepted 24 April 2022*)

Abstract−The dynamic viscosity of MWCNT-Al_2O_3 (40 : 60)/SAE50 nanofluid (NF) is investigated. NF viscosity modeling is also performed using the response surface methodology (RSM). Several different models are proposed, including modified and unmodified cubic, quartic and fifth models, and the best modeling is selected using the parameters R^2, Adjusted R^2, Predicted R^2 and Square root of the residual mean square (Std. Dev.). The results show that the fifth-order model has values of 0.9997, 0.9997, 0.9996 and 2.39 for R^2, Adjusted R^2, Predicted R^2 and Std. Dev. parameters, respectively, which indicates high accuracy of modeling. Using the perturbation diagram, it was found that among the parameters of temperature, solid volume fraction (φ) and shear rate (γ), the temperature parameter has the greatest effect on the dynamic viscosity of NF. The trend of changes in viscosity also shows that φ and γ have little effect on viscosity. Due to the importance of low viscosity in fluid flow and pumping, the optimal values of NF viscosity are presented, including dynamic viscosity equal to 108.092 cP in φ=0.063 and T=49.998 °C and γ=7,866.7786 s^{-1}.

Keywords: Optimization, Dynamic Viscosity, Oil-based Nanofluids, Alumina, Carbon Nanotubes, RSM

INTRODUCTION

The increasing of technology development and the importance and special applications of thermal engineering have caused special attention to be paid to thermal engineering. Finding fluids for better heat transfer is one of the efforts of thermal engineerins [1-5]. Nanotechnology today plays an important role in various branches of engineering sciences [6-10]. Thermal engineers have shown that adding particles to a fluid can improve its thermal performance [11-16]. These new fluids are known as NFs, which Choi named [17] and have a history of two decades [18]. NFs include base fluid and nanoparticles, which are usually base fluid, water, ethylene glycol (EG), oil, and so on. Nanoparticles are nanometer-sized metals, metal oxides, or carbon-based materials [19-26].

Tu et al. [27] studied the effects of nanoparticles use and bionic channel structure on power generation from equipment with waste energy. Angular frequency, amplitude and phase change parameters related to bionic structures were investigated. The results show that using CuO-H_2O NFs instead of base fluids can increase the hot end temperature of the thermoelectric plate by 7.19%. Tang et al. [28] investigated the thermo-hydraulics of NFs in a bionic heat sink. Fe_3O_4-water NF was also used in the presence of a magnetic field. The results show that the bionic surface by 35.4% compared to the smooth surface causes an excellent reduction of drag. Tu et al. [29] studied flow around the micro-ribbed tube in the heat exchanger. The results show that in the mass fraction of 0.4%, the heat exchanger has the highest efficiency. Hemmat Esfe et al. [30] studied mixed convection in a square cavity. The effects of nanoparticle diameter and hot barrier position on heat transfer were analyzed. The cavity was filled with Al_2O_3/water NF and had a hot barrier. The finite volume method was used for simulation and the equations were converted to code by Fortran. The results show that reducing the particle diameter at a constant Richardson number increases heat transfer. Wang et al. [31] simulated heat and flow transfer in triangular and circular tubes with internally twisted strips in the presence of SiO_2-H_2O NF. The results show that a triangular tube has better performance than a circular tube. The addition of nanoparticles to the base fluid increases the Nusselt number and flow resistance coefficient. The addition of nanoparticles changes the properties of the fluid. If two or more nanoparticles or base fluid are used to make the NF, a hybrid NF is created. Hybrid NFs have significant properties. The first study on hybrid NFs with Ag and MgO nanoparticles on NF viscosity was performed [32]. Hemmat Esfe and Sarlak [33] investigated the behavior of hybrid NF including CuO and MWCNT at 85% and 15% and 10w40 base oil. The behavior of the NF in internal combustion engine was invesyigated at φ=0.05-1% in the temperature range of 5-55 °C. The results show that at φ=1% and a temperature of 55 °C, the viscosity of the NF incrased by 43.52%. Table 1 shows some studies on μ_{nf}.

To predict the thermophysical properties of NFs such as μ_{nf}, various researchers used modeling methods such as artificial neural networks (ANNs) or experimental design methods such as RSM [40-44]. To be used in other studies and to reduce the cost of experiments, the use of modeling results can be very useful, if the results of modeling are consistent with experimental data. Hemmat Esfe et al. [45] modeled the behavior of ZrO_2-MWCNT/10W40

†To whom correspondence should be addressed.
E-mail: Toghraee@iaukhsh.ac.ir

Table 1. Some studies on μ_{nf}

Authors	NF	Result
[34]	C60-SiO_2/SAE 5W30	As the concentration increases, the dynamic viscosity of NF has an irregular trend
[35]	Al_2O_3, CuO, SiO_2 and ZnO - water	μ_{nf} increases with increasing φ. When the temperature rises, the μ_{nf} decreases.
[36]	Cu-engine oil	An increase in μ_{nf} of 37% was observed for φ=1%.
[37]	CuO-EG	μ_{nf} increases with increasing φ while decreasing with increasing temperature.
[38]	Al_2O_3/EG	The increase in μ_{nf} for NFs decreases with an increasing percentage of EG.
[39]	SiO_2-graphite/water	The highest increase in μ_{nf} was observed to 36.12% in NFs with φ=2% at T=15 °C.

NF with ANN. The neural network with 2 hidden layers and 6 neurons was selected. The parameters R2 and MSE were 0.9905 and 7.0631E-05, respectively. The RSM was used by some researchers to predict the properties of NFs. Hemmat et al. [46] in a study using RSM investigated the thermophysical properties of MWCNT-ZnO/10W40 NF. They provided a relation for predicting μ_{nf}, and the results show good accuracy of this equation.

Dynamic viscosity of MWCNT-Al_2O_3 (40 : 60)/SAE50 NF was investigated in this study. Various models, including modified and unmodified cubic, quartic and fifth modeling were proposed to predict the nanofluid viscosity using R^2, Adjusted R^2, Predicted R^2, Adeq Precision and Std. Dev, which provides the model accuracy; the best model was selected. After model was selected, it was reviewed and analyzed and various graphs including the comparsion of predicted and actual values, normal distribution and residual values were presented. Also, the effect of different parameters on the viscosity of NF was presented with a perturbation diagram. Due to the importance of optimization, the optimal value for viscosity was also presented.

MATERIALS AND METHODS

In this study, the optimization and modeling of μ_{nf} NF are investigated. For this purpose, the RSM was used. The used laboratory data are the φ=0.025 to 1%, T=25 to 50 °C and γ=666.5 to 7,998 s^{-1}.

1. RSM

Design of Experiment (DOE) was developed to fit the physical experiment model. It can also be applied to numerical experiments. The choice of test design can have a large impact on the approximate accuracy and cost of constructing the RSM. The purpose of DOE is to identify design variables that have a great impact on research [47]. One of the most reliable statistical methods to improve quality is the use of DOE methods. These methods can be used in most industries such as electronics, aerospace, automobiles, medicine, food, pharmaceuticals, chemicals and processes. The DOE method can be used in new products or optimization of systems in production. RSM is a set of statistical and mathematical techniques that are useful for developing, improving, and optimizing processes. These performance criteria or qualitative characteristics are called responses. The relationship can be written as Eq. (1):

$$y=f(\xi_1, \xi_2, \ldots, \xi_k)+\varepsilon \tag{1}$$

where $\xi_1, \xi_2, \ldots, \xi_k$ are controllable input variables. ε includes the effects such as measurement error on response, various other sources that are inherent in the processor system and so on [48]. Regression coefficients are estimated by minimizing the sum of squares of error:

$$G(a)=\sum_{p=1}^{P}\{w_p(F_p-\tilde{F}_P(a))^2\}\rightarrow \min \tag{2}$$

where w_p is the weight coefficient that shows the relative share of the main function information at the point p. In RSM, the model equation is the complete second-order equation. The second-order model can be written in the form of Eq. (3):

$$Y=\beta_0+\sum_{i=1}^{n}\beta_i x_i+\sum_{i=1}^{n}\beta_{ii}x_{ii}^2+\sum_{i<j=1}^{n}\beta_{ij}x_i x_j \tag{3}$$

where β_0, β_i, β_{ii} and β_{ij} are constant, linear, quadratic and interaction effects of regression coefficients, respectively. x_i and x_j are independent coded variables. It can be represented as a matrix in the form of Eq. (4),

$$y=X\beta+\varepsilon \tag{4}$$

Eq. (4) is solved using the least square method and the coefficients of the equations are determined [49].

2. ANOVA

By comparing the variation of the actual and predicted value, the statistical concept of a model can be examined. The sum of the squares y, SS_{tot} is calculated as Eq. (5),

$$SS_{tot}=\sum_{i=1}^{n}(y_i-y)^2 \tag{5}$$

Also, to obtain the total squares of the remaining model, proceed

Table 2. Specifications of used factors in modeling

Factor	Name	Units	Type	Minimum	Maximum	Coded low	Coded high	Mean	Std. Dev.
A	φ	%	Numeric	0.0625	1.0000	−1↔0.06	+1↔1.00	0.4479	0.3403
B	T	C	Numeric	25.00	50.00	−1↔25.00	+1↔50.00	37.93	8.38
C	γ	1/s	Numeric	666.50	7,998.00	−1↔666.50	+1↔7,998.00	4,278.62	2,083.38

Table 3. Response characteristics in NF modeling

Response	Name	Observations	Analysis	Minimum	Maximum	Mean	Std. Dev.	Ratio	Transform
R1	μ_{nf}	166	Polynomial	108.1	624	261.26	135.65	5.77	None

Table 4. ANOVA for third-degree unmodified μ_{nf} model

Source	Sum of squares	df	Mean square	F-value	p-Value	
Model	3.034E+06	19	1.597E+05	11,292.10	<0.0001	Significant
A-φ	1,151.12	1	1,151.12	81.39	<0.0001	
B-T	1.743E+05	1	1.743E+05	12,326.58	<0.0001	
C-γ	685.63	1	685.63	48.48	<0.0001	
AB	14,093.24	1	14,093.24	996.51	<0.0001	
AC	14.67	1	14.67	1.04	0.3101	
BC	813.49	1	813.49	57.52	<0.0001	
A^2	573.32	1	573.32	40.54	<0.0001	
B^2	85,789.21	1	85,789.21	6,066.00	<0.0001	
C^2	554.75	1	554.75	39.23	<0.0001	
ABC	12.49	1	12.49	0.8834	0.3488	
A^2B	403.90	1	403.90	28.56	<0.0001	
A^2C	0.3733	1	0.3733	0.0264	0.8712	
AB^2	1,963.42	1	1,963.42	138.83	<0.0001	
AC^2	1.85	1	1.85	0.1306	0.7184	
B^2C	76.15	1	76.15	5.38	0.0217	
BC^2	45.83	1	45.83	3.24	0.0739	
A^3	353.51	1	353.51	25.00	<0.0001	
B^3	2,817.11	1	2,817.11	199.19	<0.0001	
C^3	30.67	1	30.67	2.17	0.1430	
Residual	2,064.82	146	14.14			
Cor total	3.036E+06	165				

as Eq. (6):

$$SS_{res}=\sum_{i=1}^{n}(y_i-\hat{y}_i)^2 \tag{6}$$

Sum of the squares of the model is obtained by Eq. (7),

$$SS_{mod}=SS_{tot}-SS_{res} \tag{7}$$

The sum of squares is determined by the degree of freedom of the mean squares (MSs). The effects of model coefficients are also determined by the sum of their corresponding squares [50].

3. Mathematical Modeling and Regression Analysis

Data were obtained from 166 experimental experiments. For modeling, three factors affecting the μ_{nf}, namely φ, temperature and γ, were used and the type of each was considered numeric. Information about these factors and coded values is given in Table 2.

The purpose of modeling is to obtain a relation for predicting the μ_{nf}. So, there is a response variable here that is μ_{nf}. Due to the proper dispersion of the data, there was no need to use the transfer function. The considered model here is cubic. More information about the response variable is given in Table 3.

RESULTS AND DISCUSSION

Due to the lack of an accurate model for the properties of many NFs, it is difficult to calculate the μ_{nf}. In this study, models were designed that can be used to predict the μ_{nf} by modeling experimental data. Modified and unmodified cubic, quartic and fifth order models are suggested for predicting the μ_{nf} of MWCNT-Al_2O_3 (40 : 60)/SAE50 NF in T=25-50 °C, φ=0.066 to 1% and γ=666.5 to 7,998 s^{-1}. Dynamic viscosity modeling of NF using unmodified third-order modeling in Eq. (8) is:

Table 5. Related parameters to the accuracy of the unmodified cubic model for μ_{nf}

Std. Dev.	3.76	R^2	0.9993
Mean	261.26	R^2_{adj}	0.9992
C.V. %	1.44	R^2_{pre}	0.9991
		Adeq precision	394.2503

$$\begin{aligned}\text{viscosity}=\,&2{,}062.49+683.387\varphi-101.466T-0.0491085\gamma\\&-22.7746\varphi T-0.0043562\varphi\gamma+0.00136714T\gamma\\&-236.149\varphi^2+1.87085T^2+3.02721e-06\gamma^2+8.59866e\\&-05\varphi T\gamma+2.58782\varphi^2T-0.000316979\varphi^2\gamma+0.205568\varphi T^2\\&+1.06761e-07\varphi\gamma^2-1.09718e-05T^2\gamma-3.59805e\\&-08T\gamma^2+73.8935\varphi^3-0.0122962T^3-8.09197e-11\gamma^3\end{aligned} \tag{8}$$

Table 4 is related to the importance of each parameter. The significance of the modeling can be seen from the large value of F from

Table 6. ANOVA for modified third-degree μ_{nf} model

Source	Sum of squares	df	Mean square	F-value	p-value	
Model	3.034E+06	14	2.167E+05	15,320.80	<0.0001	Significant
A-φ	1,361.04	1	1,361.04	96.21	<0.0001	
B-T	1.928E+05	1	1.928E+05	13,628.63	<0.0001	
C-γ	4,344.58	1	4,344.58	307.12	<0.0001	
AB	22,470.22	1	22,470.22	1,588.43	<0.0001	
BC	900.03	1	900.03	63.62	<0.0001	
A^2	600.40	1	600.40	42.44	<0.0001	
B^2	91,829.72	1	91,829.72	6,491.49	<0.0001	
C^2	694.50	1	694.50	49.09	<0.0001	
A^2B	527.06	1	527.06	37.26	<0.0001	
AB^2	3,228.27	1	3,228.27	228.21	<0.0001	
B^2C	46.51	1	46.51	3.29	0.0718	
BC^2	266.07	1	266.07	18.81	<0.0001	
A^3	349.02	1	349.02	24.67	<0.0001	
B^3	2,927.56	1	2,927.56	206.95	<0.0001	
Residual	2,136.07	151	14.15			
Cor total	3.036E+06	165				

Table 7. Related parameters to the accuracy of the modified cubic model for μ_{nf}

Std. Dev.	3.76	R^2	0.9993
Mean	261.26	R^2_{adj}	0.9992
C.V. %	1.44	R^2_{pre}	0.9991
		Adeq precision	452.9497

11292. P-values represent the statistical aspect of the model, and where values are less than 0.05 indicates the importance of this parameter, and parameters with P-values greater than 0.1 have little importance. Therefore, the trivial parts of the model are removed.

Table 5 shows the accuracy values for unmodified cubic modeling. In this modeling, R^2=0.993 and Adjusted R^2=0.992, which indicates the high accuracy of the proposed relationship.

Table 8. ANOVA for modified fourth-degree μ_{nf} model

Source	Sum of squares	df	Mean square	F-value	p-Value	
Model	3.035E+06	20	1.518E+05	19,009.98	<0.0001	Significant
A-φ	1,386.06	1	1,386.06	173.62	<0.0001	
B-T	2.220E+05	1	2.220E+05	27,813.12	<0.0001	
C-γ	978.21	1	978.21	122.53	<0.0001	
AB	274.77	1	274.77	34.42	<0.0001	
BC	230.49	1	230.49	28.87	<0.0001	
A^2	243.40	1	243.40	30.49	<0.0001	
B^2	41,877.37	1	41,877.37	5,245.69	<0.0001	
C^2	3.20	1	3.20	0.4014	0.5274	
A^2B	605.94	1	605.94	75.90	<0.0001	
AB^2	3,425.48	1	3,425.48	429.09	<0.0001	
B^2C	567.25	1	567.25	71.06	<0.0001	
A^3	319.02	1	319.02	39.96	<0.0001	
B^3	2,579.83	1	2,579.83	323.16	<0.0001	
C^3	186.82	1	186.82	23.40	<0.0001	
A^2B^2	34.36	1	34.36	4.30	0.0398	
A^3B	248.64	1	248.64	31.15	<0.0001	
AB^3	219.90	1	219.90	27.54	<0.0001	
B^3C	75.36	1	75.36	9.44	0.0025	
A^4	414.91	1	414.91	51.97	<0.0001	
C^4	52.39	1	52.39	6.56	0.0114	
Residual	1,157.56	145	7.98			
Cor total	3.036E+06	165				

Table 9. Related parameters to the accuracy of the fourth order for μ_{nf}

Std. Dev.	2.83	R^2	0.9996
Mean	261.26	R^2_{adj}	0.9996
C.V. %	1.08	R^2_{pre}	0.9995
		Adeq precision	510.1186

By removing the ineffective parameters in unmodified third-order modeling, the equation for modified third-order modeling is obtained. Ineffective parameters are parameters that have P-value values greater than 0.1. Eq. (9) shows the modified third-order modeling and the effective parameters in the modeling along with the F-value and P-value values are shown in Table 6.

$$\begin{aligned}\text{viscosity}=&2{,}058.91+687.122\varphi-101.145\text{T}-0.04976\gamma-23.3605\varphi\text{T}\\&+0.00135007\text{T}\gamma-237.795\varphi^2+1.86838\text{T}^2+2.8946\text{e}-06\gamma^2\\&+2.60857\varphi^2\text{T}+0.21683\varphi\text{T}^2-7.73764\text{e}-06\text{T}^2\gamma-5.87962\text{e}\\&-08\text{T}\gamma^2+73.3944\varphi^3-0.0124364\text{T}^3\end{aligned}\tag{9}$$

Table 7 shows the accuracy values for modified cubic modeling. In this modeling, R^2=0.993 and Adjusted R^2=0.992, which indicates the high accuracy of the proposed relationship. Note that these values are the same as the unmodified state.

Table 11. Related parameters to the accuracy of the fifth order for μ_{nf}

Std. Dev.	2.39	R^2	0.9997
Mean	261.26	R^2_{adj}	0.9997
C.V. %	0.9153	R^2_{pre}	0.9996
		Adeq precision	554.0766

Using the RSM, modeling for the viscosity of NF can be presented as a fourth-order in terms of independent variables of temperature, φ and γ. Eq. (10) shows the fourth-order viscosity modeling, and Table 8 shows the values for ANOVA.

$$\begin{aligned}\text{viscosity}=&1{,}987.32+1{,}565.38\varphi-96.4879\text{T}-0.111791\gamma\\&-71.2226\varphi\text{T}+0.00569829\text{T}\gamma-1{,}362.83\varphi^2+1.7542\text{T}^2\\&+6.58066\text{e}-06\gamma^2+21.7113\varphi^2\text{T}+1.27348\varphi\text{T}^2\\&-0.000125503\text{T}^2\gamma+1{,}150.75\varphi^3-0.0112347\text{T}^3-8.4011\text{e}\\&-10\gamma^3-0.0897113\varphi^2\text{T}^2-7.61595\varphi^3\text{T}-0.00845971\varphi\text{T}^3\\&+9.2969\text{e}-07\text{T}^3\gamma-373.329\varphi^4+3.95928\text{e}-14\gamma^4\end{aligned}\tag{10}$$

Table 9 shows the accuracy values for modified fourth-degree modeling. In this modeling, R^2=0.996 and Adjusted R^2=0.9999, which indicates the high accuracy of the proposed relationship.

Eq. (11) is the fifth model of viscosity, and ANOVA for this model is presented in Table 10.

Table 10. ANOVA for the modified fifth-degree μ_{nf} model

Source	Sum of squares	df	Mean square	F-value	p-Value	
Model	3.036E+06	24	1.265E+05	22,116.61	<0.0001	Significant
A-φ	345.67	1	345.67	60.44	<0.0001	
B-T	89,897.06	1	89,897.06	15,719.42	<0.0001	
C-γ	988.49	1	988.49	172.85	<0.0001	
AB	305.66	1	305.66	53.45	<0.0001	
BC	247.60	1	247.60	43.30	<0.0001	
A^2	60.59	1	60.59	10.59	0.0014	
B^2	41,482.79	1	41,482.79	7,253.69	<0.0001	
C^2	2.60	1	2.60	0.4538	0.5016	
A^2B	29.40	1	29.40	5.14	0.0249	
AB^2	101.29	1	101.29	17.71	<0.0001	
B^2C	603.53	1	603.53	105.53	<0.0001	
A^3	9.44	1	9.44	1.65	0.2009	
B^3	778.75	1	778.75	136.17	<0.0001	
C^3	183.03	1	183.03	32.00	<0.0001	
A^2B^2	45.83	1	45.83	8.01	0.0053	
A^3B	215.28	1	215.28	37.64	<0.0001	
AB^3	254.88	1	254.88	44.57	<0.0001	
B^3C	79.56	1	79.56	13.91	0.0003	
A^4	113.18	1	113.18	19.79	<0.0001	
C^4	51.58	1	51.58	9.02	0.0032	
A^3B^2	80.32	1	80.32	14.04	0.0003	
A^2B^3	35.15	1	35.15	6.15	0.0143	
A^4B	227.02	1	227.02	39.70	<0.0001	
A^5	14.69	1	14.69	2.57	0.1112	
Residual	806.36	141	5.72			
Cor total	3.036E+06	165				

$$\begin{aligned}\text{viscosity}=&1{,}196.76+1{,}979.15\varphi-100.603T-0.114333\gamma\\&-57.1072\varphi T+0.00587515T\gamma-4{,}363.43\varphi^2+1.92416T^2\\&+6.53171e-06\gamma^2+85.1822\varphi^2T+0.132685\varphi T^2\\&-0.000129275T^2\gamma+6{,}056.29\varphi^3-0.0130613T^3\\&-8.35803e-10\gamma^3+0.496759\varphi^2T^2-122.297\varphi^3T\\&+0.00530403\varphi T^3+9.56764e-07T^3\gamma-3{,}229.31\varphi^4\\&+3.94251e-14\gamma^4+0.583697\varphi^3T^2-0.0136168\varphi^2T^3\\&+33.5462\varphi^4T+622.604\varphi^5\end{aligned} \tag{11}$$

Table 11 shows the accuracy values for modified fifth-degree modeling. In this modeling, R^2=0.9997 and Adjusted R^2=0.9997, which indicate the high accuracy of the proposed relationship.

Various modified and unmodified cubic, quartic, and fifth models for NF viscosity were presented and the best model was determined using R^2, R^2_{adj}, R^2_{pre}, Adeq Precision and C.V. %.

Parameter R^2: Adjusted R^2 and Predicted R^2 parameters have priority over R^2 parameter. The value of parameter R^2 can be improved with a series of synthetic expressions. In general, the closer the value of R^2 is to one, the better the modeling accuracy. In the present study, the R^2 values for the modified and unmodified cubic, quartic, and fifth models are 0.9993, 0.9993, 0.9996 and 0.9997, respectively, which indicates that the fifth-degree model is better in terms of this parameter.

Adjusted R^2 parameter: Adjusted R^2 is R-squared, which is set for the number of model parameters relative to the number of design points. One criterion of the amount of change is around the mean value. Adjusted R^2 values for modified and unmodified cubic, quartic, and fifth models were 0.9992, 0.9992, 0.9996 and 0.9997, respectively. The closer the value of Adjusted R^2 for the fifth-degree model indicates the superiority of this model over other models in this regard.

The Predicted R^2 parameter: Predicted R^2 is a criterion of how much the model predicts the amount of response. Predicted R^2 values for modified and unmodified cubic, quartic, and fifth models are 0.9991, 0.9991, 0.9995 and 0.9996, respectively, indicating the superiority of the fifth-degree model.

Std. Dev.: Square root of the residual mean square is Std. Dev. The smaller the value, the better the model. The value of this parameter is equal to 3.76, 3.76, 2.83 and 2.39 for modified and unmodified cubic, quartic and fifth models, respectively, which indicates the superiority of the fifth-degree model over other models.

According to the studies of the fifth-degree model in terms of various parameters R^2, R^2_{adj}, R^2_{pre}, Adeq Precision and Std. Dev. is superior to other models and is considered the best model [51-54].

The consistency of the obtained results from the presented relationship for the μ_{nf} with the obtained experimental data at different φ is shown in Fig. 1. The small deviation of the data from the bisector indicates that the experimental data and the obtained data from the proposed relation are placed next to each other with an acceptable difference, which indicates the high accuracy of the relation.

The graph of normal scatter is given in Fig. 2, and the more linear the scatter, the more accurate the model. If the graph is significantly nonlinear or s-shaped, then it is necessary to use transfer functions. The diagram here shows a good dispersion of the data.

Fig. 3 shows the residual graph in terms of predicted values. The residual for each variable is the difference between the observed value and the predicted value for that variable. The residuals represent an error in the model and are therefore expected to have a normal distribution and be distributed in such a way that their mean value is zero. Fig. 3 shows the appropriate state for the data.

The effect of temperature, φ and γ on μ_{nf} of MWCNT-Al_2O_3 (40 : 60)/SAE50 NF, is presented in Fig. 4. This graph, which is a perturbation in terms of the aforementioned factors, shows that the temperature has the greatest effect on μ_{nf}, while the other two

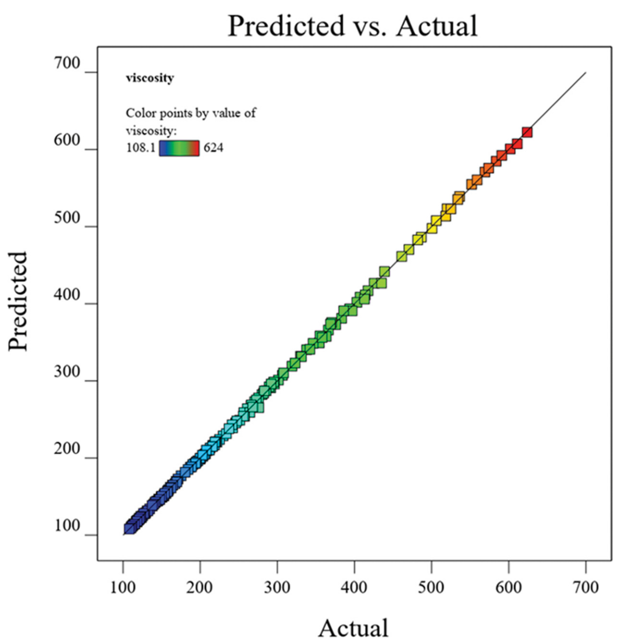

Fig. 1. Comparison of predicted and actual values.

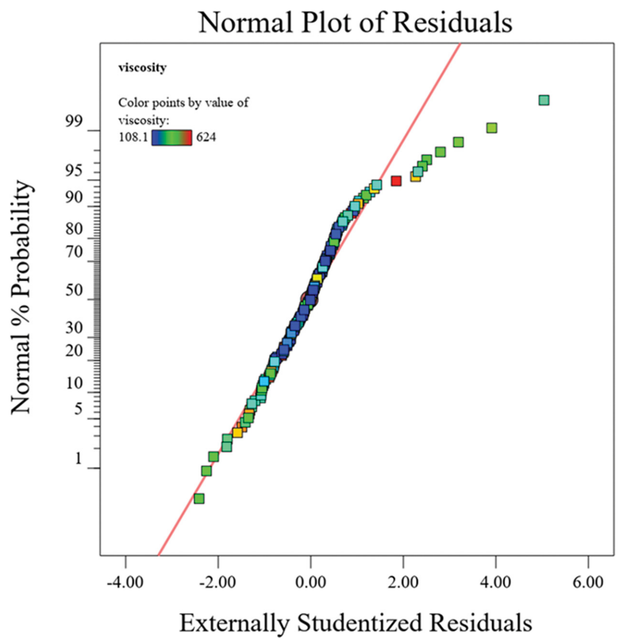

Fig. 2. Normal distribution curve versus residual values.

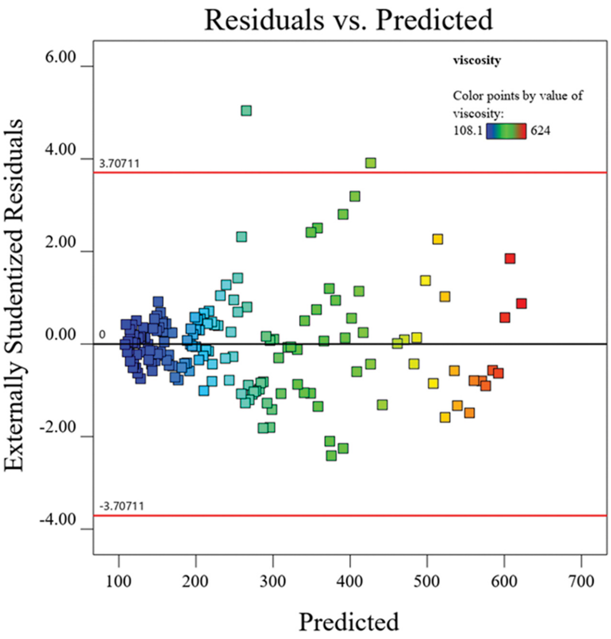

Fig. 3. Curve of predicted and remaining values.

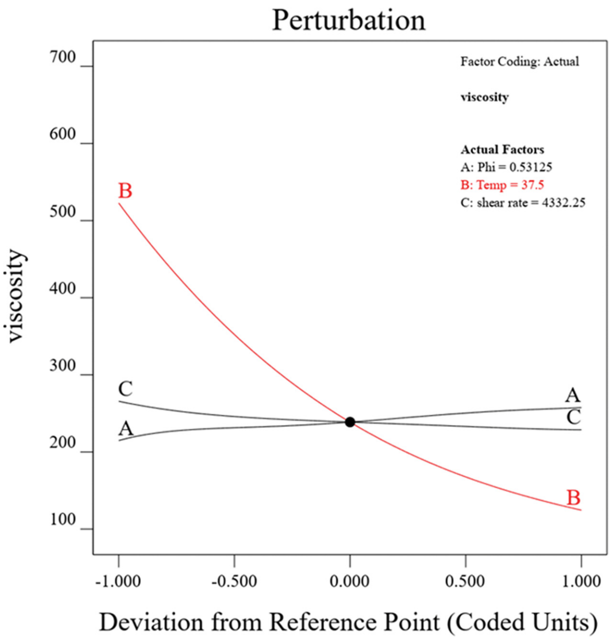

Fig. 4. Perturbation curve for effective factors.

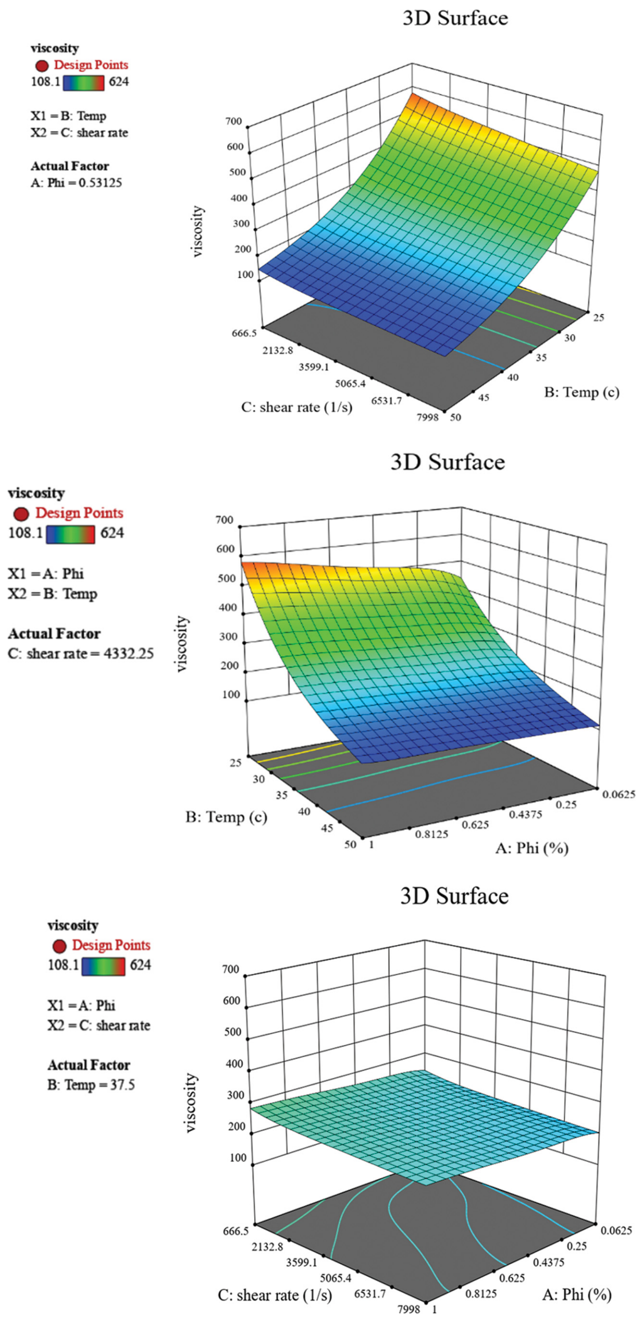

Fig. 5. The effect of different parameters on μ_{nf}.

parameters had less effect.

Also, to investigate the simultaneous effect of two parameters on the μ_{nf} of NF, the μ_{nf} curves versus temperature and φ, the μ_{nf} versus temperature and γ and μ_{nf} versus γ and φ are presented in Fig. 5. As can be seen from this figure, with increasing tempera-

Table 12. Related parameters to optimization of μ_{nf}

Name	Goal	Lower limit	Upper limit	Lower weight	Upper weight	Importance
A: φ	minimize	0.0625	1	1	1	3
B: T	is in range	25	50	1	1	3
C: γ	is in range	666.5	7,998	1	1	3
μ_{nf}	minimize	108.1	624	1	1	3

Table 13. Optimal μ_{nf} characteristics

Number	φ	T (C)	γ	μ_{nf}
1	0.063	49.998	7,666.788	108.092
2	0.063	49.996	7,893.994	108.098
3	0.063	49.998	7,867.724	108.077
4	0.063	50.000	7,738.615	108.067
5	0.063	49.995	7,766.495	108.087
6	0.063	50.000	7,959.238	108.100
7	0.063	49.996	7,808.522	108.085
8	0.063	49.995	7,820.691	108.086
9	0.063	49.998	7,897.529	108.086
10	0.063	49.998	7,597.883	108.121
11	0.063	50.000	7,632.002	108.101
12	0.063	49.997	7,995.094	108.137
13	0.063	50.000	7,510.918	108.163
14	0.063	50.000	7,481.096	108.184
15	0.063	50.000	7,433.606	108.222
16	0.063	50.000	7,351.645	108.296
17	0.063	50.000	7,306.909	108.342
18	0.063	50.000	7,278.776	108.374
19	0.063	50.000	7,251.496	108.404
20	0.063	50.000	7,223.124	108.438
21	0.063	50.000	7,196.893	108.469
22	0.063	50.000	7,109.432	108.583

ture, the μ_{nf} decreases and tends to the minimum. In addition, changes in φ and γ had little effect on μ_{nf}.

For many processes, including the pumping of fluids, low μ_{nf} is appropriate and reduces costs. In this section, the μ_{nf} is optimized. For this purpose, the settings in Table 12 were applied.

Table 13 shows the optimum points for the μ_{nf}, according to which the μ_{nf} of 108.092 cP in the φ=0.063, T=49.998 °C and γ= 7,666.788 s^{-1} is optimum.

Fig. 6 shows the optimal values for different φ and temperatures. As shown in this figure, the maximum amount of desirability occurs in the fewer φ.

CONCLUSION

The dynamic viscosity of MWCNT-Al_2O_3 (40-60)/SAE50 NF was investigated in this study. Various models for predicting viscosity using the RSM were proposed. The proposed models including modified and unmodified cubic, quartic, fifth, and ANOVA related to each model were presented. Among the proposed models, the fifth-order was more accurate because the parameters R^2, R^2_{adj}, and R^2_{pre} related to this model had a value closer to one than the other models. The values for R^2, R^2_{adj}, and R^2_{pre} for the fifth-order model are 0.9997, 0.9997 and 0.9996, respectively, which indicates the high accuracy of the model. Also, accuracy parameter of the square root of the residual mean for the fifth-order model was 2.39, which was better than the modified and unmodified cubic models, and the quartic models, which had values of 3.76, 3.76, and 2.83, respectively. The graphs of the fifth-order model, which include the predicted value curves in terms of laboratory values, normal distribution, and residual values, also confirmed the good performance of the fifth-order model. To investigate the most effective independent parameter on viscosity, the perturbation curve was used which shows that the temperature variable has the greatest effect on the dynamic viscosity of NF. The trend of changes in the dynamic viscosity of NF also showed that the viscosity of NF increases with increasing temperature. The results also show that the volume fraction and shear rate had little effect on the changes in viscosity. Due to the importance of low viscosity in fluid flow and pumping, the optimal values of NF viscosity are presented, including dynamic viscosity equal to 108.092 cP in φ=0.063 and T=49.998 °C and γ= 7,866.7786 s^{-1}.

NOMENCLATURE

MSs : mean squares

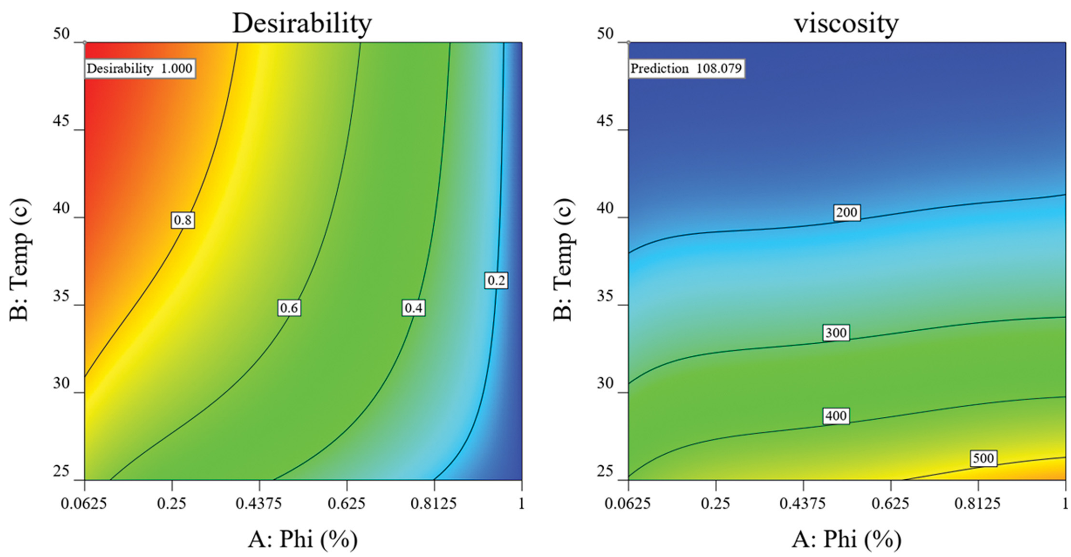

Fig. 6. Optimal values of μ_{nf} in different φ.

R^2 : regression coefficient
R^2_{adj} : adjusted regression coefficient
R^2_{pre} : predicted regression coefficient
SS_{mod} : sum of the squares of the model
SS_{tot} : sum of squares
SS_{res} : the total squares of the remaining model
T : temperature
X : independent parameter
w : weight coefficient
Y : response
y_i : acctual value
$\hat{y}_i$: predicted value

Abbreviations

ANN : artificial neural network
ANOVA : analysis of variance
DOE : design of experiment
EG : ethylene glycol
MWCNT : multi walled carbon nanotube
NF : nanofluid
RSM : response surface methodology
Std. Dev. : square root of the residual mean square

Greek Letter

ε : experimental error
ξ : controllable input variable
γ : shear rate
φ : solid volume fraction
μ : viscosity

REFERENCES

1. N. Zhang, B. Jiao, Y. Ye, Y. Kong, X. Du, R. Liu, B. Cong, L. Yu, S. Jia and K. Jia, *Energy Convers. Manag.*, **253**, 115124 (2022).
2. Y. Ye, B. Jiao, Y. Kong, R. Liu, X. Du, K. Jia, S. Yan and D. Chen, *Appl. Therm. Eng.*, **202**, 117849 (2022).
3. K. Huang, B. Su, T. Li, H. Ke, M. Lin and Q. Wang, *Appl. Therm. Eng.*, **204**, 117942 (2022).
4. L. Sun, G. Wang, C. Zhang, Q. Jin and Y. Song, *Nanotechnol. Rev.*, **10**(1), 1339 (2021).
5. Y.-M. Chu, U. Nazir, M. Sohail, M. M. Selim and J.-R. Lee, *Fractal and Fractional*, **5**(3), 119 (2021).
6. H. Li, P. Xu, D. Liu, J. He, H. Zu, J. Song, J. Zhang, F. Tian, M. Yun and F. Wang, *Nanotechnology*, **32**(37), 375202 (2021).
7. M. Cao, Z. Chang, J. Tan, X. Wang, P. Zhang, S. Lin, J. Liu and A. Li, *ACS Appl. Mater. Interfaces*, **14**(11), 13025 (2022).
8. H. Wu, F. Zhang, Z. Zhang and L. Hou, *Int. J. Multiph. Flow*, **15**, 104043 (2022).
9 Y.-M. Chu, B. M. Shankaralingappa, B. J. Gireesha, F. Alzahrani, M. Ijaz Khan and S. U. Khan, *Appl. Math. Comput.*, **419**, 126883 (2021).
10. Z. Shen, F. Wang, Z. Wang and J. Li, *Renew. Sustain. Energy Rev.*, **141**, 110783 (2021).
11. B. C. Pak and Y. I. Cho, *Exp. Heat Transf.*, **11**(2), 151 (1998).
12. A. Dezfulizadeh, A. Aghaei, A. H. Joshaghani and M. M. Najafizadeh, *Powder Technol.*, **389**, 215 (2021).
13. S. M. S. Hosseini and M. S. Dehaj, *Energy*, **234**, 121317 (2021).
14. A. Shahsavar, M. Jamei and M. Karbasi, *Powder Technol.*, **393**, 1 (2021).
15. T. T. Loong, H. Salleh, A. Khalid and H. Koten, *Case Stud. Therm. Eng.*, 101288 (2021).
16. M. H. Esfe, H. Rostamian and M. R. Sarlak, *J. Mol. Liq.*, **254**, 406 (2018).
17. S. U. S. Chol and J. A. Estman, *ASME-Publications-Fed*, **231**, 99 (1995).
18. H. D. Koca, S. Doganay, A. Turgut, I. H. Tavman, R. Saidur and I. M. Mahbubul, *Renew. Sustain. Energy Rev.*, **82**, 1664 (2018).
19. S. H. Kim, S. R. Choi and D. Kim, *J. Heat Transfer.*, **129**(3), 298 (2007).
20. V. Mikkola, S. Puupponen, H. Granbohm, K. Saari, T. Ala-Nissila and A. Seppälä, *Int. J. Therm. Sci.*, **124**, 187 (2018).
21. R. V. Pinto and F. A. S. Fiorelli, *Appl. Therm. Eng.*, **108**, 720 (2016).
22. A. Asadi, M. Asadi, A. Rezaniakolaei, L. A. Rosendahl, M. Afrand and S. Wongwises, *Int. J. Heat Mass Transf.*, **117**, 474 (2018).
23. S. Fuxi, S. Hamedi, M. Hajian, D. Toghraie, A. A. Alizadeh, M. Hekmatifar and N. Sina, *Case Stud. Therm. Eng.*, 101293 (2021).
24. X. Yang, A. Boroomandpour, S. Wen, D. Toghraie and F. Soltani, *Powder Technol.*, **388**, 418 (2021).
25. S. R. Nfawa, A. A. Basri and S. U. Masuri, *Case Stud. Therm. Eng.*, 101279 (2021).
26. G. Coccia, S. Tomassetti and G. Di Nicola, *Renew. Sust. Energ. Rev.*, **151**, 111573 (2021).
27. J. Tu, C. Qi, Z. Tang, Z. Tian and L. Chen, *Appl. Therm. Eng.*, **202**, 117893 (2022).
28. J. Tang, C. Qi, Z. Ding, M. Afrand and Y. Yan, *Int. Commun. Heat Mass Transf.*, **127**, 105492 (2021).
29. J. Tu, C. Qi, K. Li and Z. Tang, *Powder Technol.*, **395**, 562 (2022).
30. M. Hemmat Esfe, S. S. M. Esforjani, M. Akbari and A. Karimipour, *Heat Transf. Res.*, **45**(6), 563 (2014).
31. Y. Wang, C. Qi, Z. Ding, J. Tu and R. Zhao, *Powder Technol.*, **392**, 570 (2021).
32. M. Hemmat Esfe, A. A. A. Arani, M. Rezaie, W. M. Yan and A. Karimipour, *Int. Commun. Heat Mass Transf.*, **66**, 189 (2015).
33. M. Hemmat Esfe, H. Rostamian, M. Rejvani and M. R. S. Emami, *Physica E Low Dimens. Syst. Nanostruct.*, **102**, 160 (2018).
34. S. H. Rostamian, S. Saedodin, S. A. Asgari and A. H. Salarian, *J. Therm. Anal. Calorim.*, **147**, 155 (2020).
35. O. A. Alawi, N. A. C. Sidik, H. W. Xian, T. H. Kean and S. N. Kazi, *Int. J. Heat Mass Transf.*, **116**, 1314 (2018).
36. S. Aberoumand and A. Jafarimoghaddam, *J. Taiwan Inst. Chem. Eng.*, **71**, 315 (2017).
37. M. Hemmat Esfe, M. Bahiraei and O. Mahian, *Powder Technol.*, **338**, 383 (2018).
38. H. W. Chiam, W. H. Azmi, N. A. Usri, R. Mamat and N. M. Adam, *Exp. Therm. Fluid Sci.*, **81**, 420 (2017).
39. A. S. Dalkılıç, Ö. Açıkgöz, B. O. Küçükyıldırım, A. A. Eker, B. Lüleci, C. Jumpholkul and S. Wongwises, *Int. Commun. Heat Mass Transf.*, **97**, 30 (2018).
40. M. Hemmat Esfe, *Appl. Therm. Eng.*, **126**, 559 (2017).
41. A. Abdulrahman, *Mater. Today: Proc.*, **42**, 771 (2021).
42. Y. M. Chu, M. Ibrahim, T. Saeed, A. S. Berrouk, E. A. Algehyne and R. Kalbasi, *J. Mol. Liq.*, **333**, 115969 (2021).
43. Y. Cao, A. Khan, A. Abdi and M. Ghadiri, *Arab. J. Chem.*, **14**(7),

103204 (2021).
44. W. Ji, L. Yang, Z. Chen, M. Mao and J. N. Huang, *Powder Technol.*, **388**, 212 (2021).
45. M. Hemmat Esfe and M. R. Sarlak, *J. Mol. Liq.*, **242**, 326 (2017).
46. M. Hemmat Esfe, S. Esfandeh and S. Niazi, *J. Mol. Liq.*, **288**, 111020 (2019).
47. L. Eriksson, E. Johansson, N. Kettaneh-Wold, C. Wikström and S. Wold, *Design of experiments, Principles and applications*, Learn ways AB, Stockholm (2000).
48. R. H. Myers, D. C. Montgomery and C. M. Anderson-Cook, *Response surface methodology: process and product optimization using designed experiments*, John Wiley & Sons (2016).
49. M. Ghafarzadeh, R. Abedini and R. Rajabi, *J. Clean. Prod.*, **150**, 361 (2017).
50. M. Mäkelä, *Energy Convers. Manag.*, **151**, 630 (2017).
51. T.-H. Zhao, M. I. Khan and Y.-M. Chu, *Math. Methods Appl. Sci.*, In press (2021), https://doi.org/10.1002/mma.7310.
52. T.-H. Zhao, O. Castillo, H. Jahanshahi, A. Yusuf, M. O. Alassafi, F. E. Alsaadi and Y.-M. Chu, *Appl. Comput. Math.*, **20**(1), 160 (2021).
53. F.-Z. Wang, M. N. Khan, I. Ahmad, H. Ahmad, H. Abu-Zinadah and Y. M. Chu, *Fractals*, **30**(2), 224005 (2022).
54. M. Nazeer, F. Hussain, M. Ijaz Khan, Asad-ur-Rehman, E. R. El-Zahar, Y.-M. Chu and M. Y. Malik, *Appl. Math. Comput.*, **420**, 126868 (2021).